

# A Belief Propagation Approach for Direct Multipath-Based SLAM

Mingchao Liang\*, Erik Leitinger<sup>†</sup>, and Florian Meyer\*

\*Department of Electrical and Computer Engineering, University of California San Diego, USA  
{m3liang, flmeyer}@ucsd.edu

<sup>†</sup>Signal Processing and Speech Communication Laboratory, Graz University of Technology, Austria  
erik.leitinger@tugraz.at

**Abstract**—In this work, we develop a multipath-based simultaneous localization and mapping (SLAM) method that can directly be applied to received radio signals. In existing multipath-based SLAM approaches, a channel estimator is used as a preprocessing stage that reduces data flow and computational complexity by extracting features related to multipath components (MPCs). We aim to avoid any preprocessing stage that may lead to a loss of relevant information. The presented method relies on a new statistical model for the data generation process of the received radio signal that can be represented by a factor graph. This factor graph is the starting point for the development of an efficient belief propagation (BP) method for multipath-based SLAM that directly uses received radio signals as measurements. Simulation results in a realistic scenario with a single-input single-output (SISO) channel demonstrate that the proposed direct method for radio-based SLAM outperforms state-of-the-art methods that rely on a channel estimator.

**Index Terms**—Simultaneous localization and mapping, SLAM, multipath channel, belief propagation, and factor graph.

## I. INTRODUCTION

Situational awareness in the indoor environment is critical in various applications, including autonomous navigation, public safety, and asset tracking. Multipath-based simultaneous localization and mapping (SLAM) is a promising approach to estimating the positions of mobile users and features in the propagation environment. By associating multipath components (MPCs) in radio signals with the geometry of the radio reflectors, multipath propagation is exploited to increase positioning accuracy and build a partial map of the indoor environment. Conventional multipath-based SLAM methods [1]–[6] use a channel estimator [7]–[10] to detect and extract MPCs by preprocess received radio signals in blocks of samples or “snapshots”. The parameters of each extracted MPC include delay, angle of arrival, and angle of departure. These parameters are used as noisy measurements for a SLAM method that is based on belief propagation (BP) [1]–[4], Rao-Blackwellized particle filtering [5], or neural networks [6]. This two-step processing is widely used as it reduces data flow and, thus, the computational complexity of SLAM. However, important information may be lost in this preprocessing stage. In particular, if parameters of multiple MPCs are very similar the channel estimator may detect them as a single MPC due to finite resolution capabilities limited by signal bandwidth. This can lead to a significantly degraded SLAM performance.

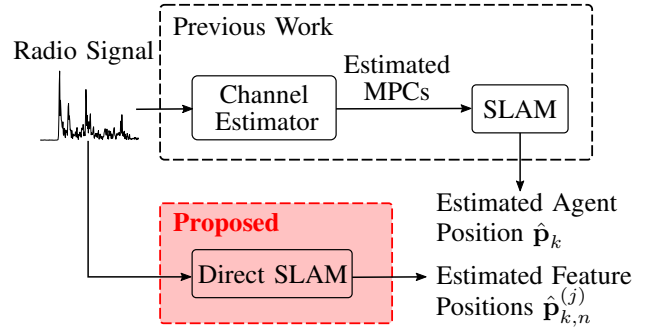


Fig. 1: Flow diagram of the proposed direct multipath-based SLAM that uses the received radio signal as measurements. A flow diagram of conventional multipath-based SLAM that uses the estimated MPCs provided by the channel estimator as measurements is also shown.

In this paper, we propose a multipath-based SLAM method for single-input single-output (SISO) systems that avoids any preprocessing stage by directly using received radio signals as measurements. Our approach addresses direct multipath-based SLAM as a joint sequential Bayesian inference problem. Fig. 1 shows the flow diagram of the proposed direct method compared to existing methods with a channel estimator.

For direct SLAM, we introduce a new statistical model to describe the data-generating process of received radio signals, which is a combination of the Swerling 1 model for correlated measurements in [11] and Bernoulli existence model in [12]. This statistical model can be represented well by a factor graph [13], [14]. Based on the factor graph, an efficient sequential BP message-passing method for the estimation of mobile agent position and features in the propagation environment is developed. For an accurate approximation of BP messages, following our previous work in [12], [15], [16], we represent some of the BP messages by random samples “particles” and others by a mean and covariance matrix obtained via moment matching. The main contributions of this work are summarized as follows.

- We introduce a new statistical model for multipath-based SLAM using received radio signals.
- We develop an efficient BP method for direct multipath-based SLAM.

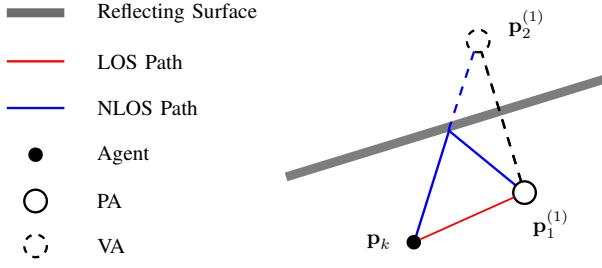


Fig. 2: Scenario with one mobile agent, one physical anchor (PA), and one virtual anchor (VA).

By comparing the proposed direct approach with a state-of-the-art reference method for multipath-based SLAM, we demonstrate that directly using the received radio signal as a measurement can lead to an improved SLAM performance.

## II. SYSTEM MODEL

For multipath-based SLAM, we consider a mobile agent with an unknown time-varying position  $\mathbf{p}_k \in \mathbb{R}^2$  and  $J$  physical anchors (PAs) with known positions  $\mathbf{p}_1^{(j)} \in \mathbb{R}^2, j \in \{1, \dots, J\}$ , where  $k$  is the index of discrete time. The number of physical anchors,  $J$ , is assumed to be known. There are  $L_k^{(j)} - 1$  virtual anchors (VAs) with unknown position  $\mathbf{p}_l^{(j)} \in \mathbb{R}^2, l = \{2, \dots, L_k^{(j)}\}$  associated to the  $j$ -th PA. The number of VAs,  $L_k^{(j)}$ , is time-varying and unknown. VAs are the mirror images of the PA at reflecting surfaces. Fig. 2 shows a scenario with one PA and one VA.

The number of VAs  $L_k^{(j)}$  is time-varying and unknown. To address this, at each discrete time step  $k$ , we introduce potential features (PF) [17] indexed by  $(j, n), j \in \{1, \dots, J\}, n \in \{1, \dots, N_k^{(j)}\}$ . The existence of each PFs is modeled by binary random variables  $r_{k,n}^{(j)} \in \{0, 1\}, j \in \{1, \dots, J\}, n \in \{1, \dots, N_k^{(j)}\}$ . Here  $N_k^{(j)}$  is the maximum possible number of features at time step  $k$ , i.e.,  $N_k^{(j)} \geq L_k^{(j)}$ . The state of a PF is denoted by  $\mathbf{y}_{k,n}^{(j)}$ , which includes their position  $\mathbf{p}_{k,n}^{(j)}$ , existence  $r_{k,n}^{(j)}$ , and intensity  $\gamma_{k,n}^{(j)}$ . We further introduce the notation  $\phi_{k,n}^{(j)} = [\mathbf{p}_{k,n}^{(j)\top} \gamma_{k,n}^{(j)}]^\top$ . Note that PAs are also represented by PFs since their intensity is also time-varying, and line of sight (LOS) paths to PAs may be unavailable. The state of the mobile agent is denoted as  $\mathbf{x}_k$ . It includes the agent's position  $\mathbf{p}_k$  and possibly further motion-related parameters. For future reference, we establish the notation  $\mathbf{y}_k^{(j)} = [\mathbf{y}_{k,1}^{(j)\top} \dots \mathbf{y}_{k,N_k^{(j)}}^{(j)\top}]^\top$ .

### A. Measurement Model

We consider a SISO system, where at each time  $k$ , the mobile agent transmits a radio signal, which is received by the PAs. However, note that the proposed model can be easily reformulated for the case where the PAs act as transmitters and the mobile agent act as a receiver. Let  $H(f)$  be the frequency-domain representation of the transmitted radio signal in the baseband. The total bandwidth of the signal is denoted as  $B$ . The radio signal received by the  $j$ -th PA can now be modeled as [18, Ch. 2]

$$Z_k^{(j)}(f) = \sum_{l=1}^{L_k^{(j)}} \rho_{k,l}^{(j)} H(f) e^{-j2\pi f \tau_{k,l}^{(j)}} + \epsilon_k^{(j)}(f). \quad (1)$$

Here,  $\rho_{k,l}^{(j)} \in \mathbb{C}$  and  $\tau_{k,l}^{(j)} = \|\mathbf{p}_k - \mathbf{p}_l^{(j)}\|/c$  are the complex amplitude and the delay related to the  $l$ -th propagation path and  $c$  is the speed of light. The complex amplitude  $\rho_{k,n}^{(j)}$  is distributed according to a circularly symmetric complex Gaussian probability density function (PDF). Specifically, the absolute value of  $\rho_{k,n}^{(j)}$  is Rayleigh distributed and its phase is uniformly distributed over  $[0, 2\pi)$ . The complex amplitudes  $\rho_{k,l}^{(j)}$  and  $\rho_{k,l'}^{(j')}$  are independent if  $(k, l, j) \neq (k', l', j')$ . This amplitude model is also known as *Swerling 1* [11], [19].

The first term on the right-hand side of (1) describes the contribution of the PA from the LOS path and the contributions of VAs from the non-line of sight (NLOS) paths due to specular reflections. The complex additive noise  $\epsilon_k^{(j)}(f)$  aggregates measurement noise, diffuse multipath components, and specular paths that cannot be resolved with the available bandwidth. The noise is assumed to be a zero-mean, uncorrelated, circularly-symmetric complex Gaussian process [20]–[22].

Sampling the received signal  $Z_k^{(j)}(f)$  with frequency spacing  $\Delta$  leads to the measurement vector  $\mathbf{z}_k^{(j)} = [z_{k,1}^{(j)} \dots z_{k,M}^{(j)}]^\top = [z_k^{(j)}(-\frac{(M-1)\Delta}{2}) \dots z_k^{(j)}(\frac{(M-1)\Delta}{2})]^\top \in \mathbb{C}^M$  with length  $M = B/\Delta + 1$ . We can now express the signal model in (1) in terms of PF states  $\mathbf{y}_{k,n}^{(j)} = [\mathbf{p}_{k,n}^{(j)\top} \gamma_{k,n}^{(j)} r_{k,n}^{(j)}]^\top$ , i.e.,

$$\mathbf{z}_k^{(j)} = \sum_{n=1}^{N_k^{(j)}} r_{k,n}^{(j)} \rho_{k,n}^{(j)} \mathbf{h}_{k,n}^{(j)} + \epsilon_k^{(j)} \quad (2)$$

with  $\epsilon_k^{(j)} = [\epsilon_k^{(j)}(-\frac{(M-1)\Delta}{2}) \dots \epsilon_k^{(j)}(\frac{(M-1)\Delta}{2})]^\top \in \mathbb{C}^M$ . Here, the vector  $\mathbf{h}_{k,n}^{(j)} \in \mathbb{C}^M$  represents the sampled transmit signal, i.e.,

$$\mathbf{h}_{k,n}^{(j)} = \left[ H\left(\frac{-(M-1)\Delta}{2}\right) e^{-j2\pi\left(\frac{-(M-1)\Delta}{2}\right)\tau_{k,n}^{(j)}} \dots H\left(\frac{(M-1)\Delta}{2}\right) e^{-j2\pi\left(\frac{(M-1)\Delta}{2}\right)\tau_{k,n}^{(j)}} \right]^\top. \quad (3)$$

Recall that  $\tau_{k,n}^{(j)} = \|\mathbf{p}_k - \mathbf{p}_{k,n}^{(j)}\|/c$ . Based on assumptions made above, the complex amplitude  $\rho_{k,n}^{(j)}$  is distributed according to  $\mathcal{CN}(\rho_{k,n}^{(j)}; 0, \gamma_{k,n}^{(j)})$ , and the noise  $\epsilon_k^{(j)}$  is distributed according to  $\mathcal{CN}(\epsilon_k^{(j)}; \mathbf{0}, \mathbf{C}_\epsilon^{(j)})$ . The noise covariance matrix  $\mathbf{C}_\epsilon^{(j)}$  is assumed unknown and is modeled as a random variable. It can be easily verified that the conditional PDF  $f(\mathbf{z}_k^{(j)} | \mathbf{x}_k, \mathbf{y}_k^{(j)}, \mathbf{C}_\epsilon^{(j)})$  is also zero-mean complex Gaussian with covariance matrix  $\mathbf{C}_k^{(j)} = \mathbf{C}_\epsilon^{(j)} + \sum_{n=1}^{N_k^{(j)}} r_{k,n}^{(j)} \gamma_{k,n}^{(j)} \mathbf{h}_{k,n}^{(j)} \mathbf{h}_{k,n}^{(j)\text{H}}$ .

### B. State-Transition Model

The evolution of the agent state  $\mathbf{x}_k$ , PF states  $\mathbf{y}_{k,n}^{(j)}$  and the noise covariance  $\mathbf{C}_{\epsilon,k}^{(j)}$  are assumed to be independent across  $k, j$ , and  $n$  and are described by the state transition PDFs  $f(\mathbf{x}_k | \mathbf{x}_{k-1}), f(\mathbf{y}_{k,n}^{(j)} | \mathbf{y}_{k,n-1}^{(j)}) = f(\phi_{k,n}^{(j)} | \phi_{k,n-1}^{(j)}, r_{k,n}^{(j)} | r_{k,n-1}^{(j)})$ , and  $f(\mathbf{C}_{\epsilon,k}^{(j)} | \mathbf{C}_{\epsilon,k-1}^{(j)})$ , respectively. Specifically, if legacy

PF  $n \in \{1, \dots, N_{k-1}^{(j)}\}$  does not exist at  $k-1$ , i.e.,  $r_{k,n-1}^{(j)} = 0$ , then it does not exist at  $k$  either. The state-transition PDF thus reads  $f(\phi_{k,n}^{(j)}, 1 | \phi_{k,n-1}^{(j)}, 0) = 0$  and  $f(\phi_{k,n}^{(j)}, 0 | \phi_{k,n-1}^{(j)}, 0) = f_D(\phi_{k,n}^{(j)})$  with  $f_D(\cdot)$  being an arbitrary ‘‘dummy’’ PDF. If PF  $n$  exists at  $k-1$ , i.e.,  $r_{k,n-1}^{(j)} = 1$ , then the probability that it also exists at  $k$ , is  $p_s$ , known as the survival probability. The state-transition PDF reads  $f(\phi_{k,n}^{(j)}, 1 | \phi_{k,n-1}^{(j)}, 1) = p_s f(\phi_{k,n}^{(j)} | \phi_{k,n-1}^{(j)})$  and  $f(\phi_{k,n}^{(j)}, 0 | \phi_{k,n-1}^{(j)}, 1) = (1 - p_s) f_D(\phi_{k,n}^{(j)})$ .

The birth of newly appearing features associated with PA  $j$  at time  $k$ , is modeled by a Poisson point process with mean  $\mu_B^{(j)}$  and spatial PDF  $f_B^{(j)}(\phi | \mathbf{x}_k)$ . Based on the assumption that the number of newly appearing features is significantly smaller than the number of measurements,  $M$ , we introduce  $M$  new PFs, one for each measurement  $z_{k,m}^{(j)}$  [12]. Thus,  $N_k^{(j)} = N_{k-1}^{(j)} + M$  [12]. Let  $\mathcal{P}_m(\mathbf{x}_k)$  be the region occupied by measurement  $m \in \{1, \dots, M\}$  that is defined as

$$\mathcal{P}_m(\mathbf{x}_k) = \{\mathbf{p} \mid (m-1)T_s \leq \|\mathbf{p} - \mathbf{p}_k\|/c \leq mT_s\}$$

with  $T_s = 1/\Delta$ . The birth PDF of new PF  $n = N_{k-1}^{(j)} + m$ , is  $f_{B,n}^{(j)}(\phi_{k,n}^{(j)} | \mathbf{x}_k) \propto f_B^{(j)}(\phi | \mathbf{x}_k)$  if  $\mathbf{p}_{k,n} \in \mathcal{P}_m(\mathbf{x}_k)$ , and zero otherwise.

To define the birth probability, we first note that the number of new features in cell  $\mathcal{P}_m(\mathbf{x}_k)$  is also Poisson distributed with mean  $\mu_{B,n}^{(j)} = \mu_B^{(j)} \int \int_{\mathcal{P}_m(\mathbf{x}_k)} f_B^{(j)}(\phi | \mathbf{x}_k) d\mathbf{p} d\gamma$ . By assuming that there is at most one new feature in cell  $\mathcal{P}_m(\mathbf{x}_k)$ , we obtain  $p_{B,n}^{(j)} = \mu_{B,n}^{(j)} / (\mu_{B,n}^{(j)} + 1)$ . The prior PDF  $f(\mathbf{y}_{k,n}^{(j)} | \mathbf{x}_k) = f(\phi_{k,n}^{(j)}, r_{k,n}^{(j)} | \mathbf{x}_k)$  for individual new PFs thus reads  $f(\phi_{k,n}^{(j)}, 0 | \mathbf{x}_k) = (1 - p_{B,n}^{(j)}) f_D(\phi_{k,n}^{(j)})$  and  $f(\phi_{k,n}^{(j)}, 1 | \mathbf{x}_k) = p_{B,n}^{(j)} f_B^{(j)}(\phi_{k,n}^{(j)} | \mathbf{x}_k)$ . As a result of the Poisson point process assumption for newly appearing features, the new PF can be assumed statistically independent.

### C. The Factor Graph

Based on the introduced statistical models and further common assumptions [17], the joint posterior PDF  $f(\mathbf{x}_{0:k}, \mathbf{y}_{0:k} | \mathbf{z}_{1:k})$  can then be factorized as

$$\begin{aligned} & f(\mathbf{x}_{0:k}, \mathbf{y}_{0:k}, \mathbf{C}_{\epsilon,0:k} | \mathbf{z}_{1:k}) \\ & \propto f(\mathbf{x}_0) \left( \prod_{j=1}^J f(\mathbf{C}_{\epsilon,0}^{(j)}) \prod_{n=1}^{N_0^{(j)}} f(\mathbf{y}_{0,n}^{(j)}) \right) \prod_{k'=1}^k f(\mathbf{x}_{k'} | \mathbf{x}_{k'-1}) \\ & \times \prod_{j=1}^J \left( \prod_{n=1}^{N_{k'-1}^{(j)}} f(\mathbf{y}_{k',n}^{(j)} | \mathbf{y}_{k'-1,n}^{(j)}) \right) \left( \prod_{n=N_{k'-1}^{(j)}+1}^{N_{k'}^{(j)}} f(\mathbf{y}_{k',n}^{(j)} | \mathbf{x}_{k'}) \right) \\ & \times f(\mathbf{C}_{\epsilon,k'}^{(j)} | \mathbf{C}_{\epsilon,k'-1}^{(j)}) f(\mathbf{z}_{k'}^{(j)} | \mathbf{x}_{k'}, \mathbf{y}_{k'}^{(j)}, \mathbf{C}_{\epsilon,k'}^{(j)}) \end{aligned} \quad (4)$$

where we introduced  $\mathbf{x}_{0:k} \triangleq [\mathbf{x}_0^T \dots \mathbf{x}_k^T]^T$ ,  $\mathbf{y}_{0:k} \triangleq [\mathbf{y}_0^T \dots \mathbf{y}_k^T]^T$ ,  $\mathbf{y}_k \triangleq [\mathbf{y}_k^{(1)T} \dots \mathbf{y}_k^{(J)T}]^T$ ,  $\mathbf{C}_{\epsilon,k} \triangleq [\mathbf{C}_{\epsilon,k}^{(1)} \dots \mathbf{C}_{\epsilon,k}^{(J)}]$ , and  $\mathbf{C}_{\epsilon,0:k} \triangleq [\mathbf{C}_{\epsilon,0} \dots \mathbf{C}_{\epsilon,k}]$ . Note that measurement vector  $\mathbf{z}_{1:k}$  is here assumed observed and thus fixed. Based on the factorization in (4),  $f(\mathbf{x}_{0:k}, \mathbf{y}_{0:k}, \mathbf{C}_{\epsilon,0:k} | \mathbf{z}_{1:k})$  can be represented by the factor graph [14] shown in Fig. 3 for a single step

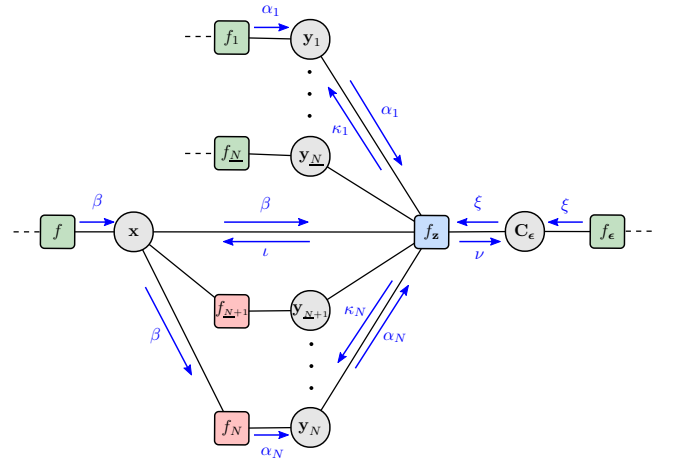


Fig. 3: Factor graph used for the development of the proposed direct SLAM method. A single time step  $k$  and a single PA  $j$  are shown. The indexes  $k$  and  $j$  are omitted and the following shorthand notations are used:  $\underline{N} = N_{k-1}^{(j)}$ ,  $N = N_k^{(j)}$ ,  $\mathbf{x} = \mathbf{x}_k$ ,  $\mathbf{y}_n = \mathbf{y}_{k,n}^{(j)}$ ,  $\mathbf{C}_\epsilon = \mathbf{C}_{\epsilon,k}^{(j)}$ ,  $f_z = f(\mathbf{z}_k^{(j)} | \mathbf{x}_k, \mathbf{y}_k^{(j)}, \mathbf{C}_{\epsilon,k}^{(j)})$ ,  $f = f(\mathbf{x}_k | \mathbf{x}_{k-1})$ ,  $f_\epsilon = f(\mathbf{C}_{\epsilon,k}^{(j)} | \mathbf{C}_{\epsilon,k-1}^{(j)})$ ,  $f_n = f(\mathbf{y}_{k,n}^{(j)} | \mathbf{y}_{k-1,n}^{(j)})$  for  $n \in \{1, \dots, N_{k-1}^{(j)}\}$ , and  $f_n = f(\mathbf{y}_{k,n}^{(j)} | \mathbf{x}_k)$  for  $n \in \{N_{k-1}^{(j)} + 1, \dots, N_k^{(j)}\}$ . Moreover,  $\beta = \beta(\mathbf{x}_k)$ ,  $\alpha_n = \alpha(\mathbf{y}_{k,n}^{(j)})$ ,  $\xi = \xi(\mathbf{C}_{\epsilon,k}^{(j)})$ ,  $l = l(\mathbf{x}_k; \mathbf{z}_k^{(j)})$ ,  $\kappa_n = \kappa(\mathbf{y}_{k,n}^{(j)}; \mathbf{z}_k^{(j)})$ , and  $\nu = \nu(\mathbf{C}_{\epsilon,k}^{(j)}; \mathbf{z}_k^{(j)})$ .

and a single PA. Note that contrary to previous work [12], the individual measurements  $z_{k,m}^{(j)}$ ,  $m \in \{1, \dots, M\}$  are coherent and thus not independent conditioned on  $\mathbf{x}_k$ ,  $\mathbf{y}_k^{(j)}$ , and  $\mathbf{C}_{\epsilon,k}^{(j)}$ . In contrast to [12, Eq. (2)], it is thus not possible to factorize the joint likelihood function  $f(\mathbf{z}_k^{(j)} | \mathbf{x}_k, \mathbf{y}_k^{(j)}, \mathbf{C}_{\epsilon,k}^{(j)})$  into individual likelihood functions for measurements  $z_{k,m}^{(j)}$ ,  $m \in \{1, \dots, M\}$ .

## III. THE PROPOSED BELIEF PROPAGATION (BP) METHOD

This section introduces the proposed BP method for direct SLAM. BP is an efficient technique to compute approximate marginal posterior PDFs, also known as beliefs, in terms of the sum-product rule by performing local operations, so-called ‘‘messages’’, passed along the edges of a factor graph. Since the factor graph of the considered direct SLAM problem has loops, there is no fixed message passing order [13], [14]. We apply the following message passing schedule: (i) messages are only passed forward in time, (ii) along the edges connecting an agent state variable node ‘‘ $\mathbf{x}_k$ ’’ and a new PF state variable node ‘‘ $\mathbf{y}_{k,n}^{(j)}$ ’’, messages are only sent from the former to the latter [1].

### A. BP Message Passing

Following the sum-product message passing rules, we first compute the prediction messages  $\beta(\mathbf{x}_k)$ ,  $\xi(\mathbf{C}_{\epsilon,k}^{(j)})$ , and  $\alpha(\mathbf{y}_{k,n}^{(j)})$ , for  $n \in \{1, \dots, N_{k-1}^{(j)}\}$ . These messages are obtained based on beliefs from the previous time step and the state-transition models introduced in Section II-B, i.e.,

$$\begin{aligned}\beta(\mathbf{x}_k) &= \int f(\mathbf{x}_k|\mathbf{x}_{k-1})\tilde{f}(\mathbf{x}_{k-1})d\mathbf{x}_{k-1} \\ \xi(\mathbf{C}_{\epsilon,k}^{(j)}) &= \int f(\mathbf{C}_{\epsilon,k}^{(j)}|\mathbf{C}_{\epsilon,k-1}^{(j)})\tilde{f}(\mathbf{C}_{\epsilon,k-1}^{(j)})d\mathbf{C}_{\epsilon,k-1}^{(j)} \\ \alpha(\mathbf{y}_{k,n}^{(j)}) &= \sum_{\mathbf{y}_{k-1,n}^{(j)}} f(\mathbf{y}_{k,n}^{(j)}|\mathbf{y}_{k-1,n}^{(j)})\tilde{f}(\mathbf{y}_{k-1,n}^{(j)})\end{aligned}$$

where  $\sum_{\mathbf{y}_{k-1,n}^{(j)}}$  denotes ‘‘marginalizing out’’  $\mathbf{y}_{k-1,n}^{(j)}$ . This marginalization includes the summation over  $r_{k-1,n}^{(j)}$  and the integration over  $\mathbf{p}_{k-1,n}^{(j)}$  and  $\gamma_{k-1,n}^{(j)}$ . Here,  $\tilde{f}(\mathbf{x}_{k-1})$ ,  $\tilde{f}(\mathbf{C}_{\epsilon,k-1}^{(j)})$ , and  $\tilde{f}(\mathbf{y}_{k-1,n}^{(j)})$  are the beliefs computed at the previous time step. For the new PFs  $n \in \{N_{k-1}^{(j)} + 1, \dots, N_k^{(j)}\}$ , since we only pass from ‘‘ $\mathbf{x}_k$ ’’ to ‘‘ $\mathbf{y}_{k,n}^{(j)}$ ’’, the corresponding ‘‘birth messages’’ are given by  $\alpha(\mathbf{y}_{k,n}^{(j)}) = \int f(\mathbf{y}_{k,n}^{(j)}|\mathbf{x}_k)\beta(\mathbf{x}_k)d\mathbf{x}_k$ .

Furthermore, based on sum-product message passing rules, the measurement update messages  $\iota(\mathbf{x}_k; \mathbf{z}_k^{(j)})$ ,  $\nu(\mathbf{C}_{\epsilon,k}^{(j)}; \mathbf{z}_k^{(j)})$ , and  $\kappa(\mathbf{y}_{k,n}^{(j)}; \mathbf{z}_k^{(j)})$  that introduce the information of the current measurement  $\mathbf{z}_k^{(j)}$ , can be obtained as

$$\begin{aligned}\iota(\mathbf{x}_k; \mathbf{z}_k^{(j)}) &= \sum_{\mathbf{y}_k^{(j)}} \int f(\mathbf{z}_k^{(j)}|\mathbf{x}_k, \mathbf{y}_k^{(j)}, \mathbf{C}_{\epsilon,k}^{(j)})\xi(\mathbf{C}_{\epsilon,k}^{(j)}) \\ &\quad \times \prod_{n=1}^{N_k^{(j)}} \alpha(\mathbf{y}_{k,n}^{(j)})d\mathbf{C}_{\epsilon,k}^{(j)}\end{aligned}\quad (5)$$

$$\begin{aligned}\nu(\mathbf{C}_{\epsilon,k}^{(j)}; \mathbf{z}_k^{(j)}) &= \sum_{\mathbf{y}_k^{(j)}} \int f(\mathbf{z}_k^{(j)}|\mathbf{x}_k, \mathbf{y}_k^{(j)}, \mathbf{C}_{\epsilon,k}^{(j)})\beta(\mathbf{x}_k) \\ &\quad \times \prod_{n=1}^{N_k^{(j)}} \alpha(\mathbf{y}_{k,n}^{(j)})d\mathbf{x}_k.\end{aligned}\quad (6)$$

$$\begin{aligned}\kappa(\mathbf{y}_{k,n}^{(j)}; \mathbf{z}_k^{(j)}) &= \sum_{\mathbf{y}_k^{(j)} \setminus \mathbf{y}_{k,n}^{(j)}} \iint f(\mathbf{z}_k^{(j)}|\mathbf{x}_k, \mathbf{y}_k^{(j)}, \mathbf{C}_{\epsilon,k}^{(j)})\xi(\mathbf{C}_{\epsilon,k}^{(j)}) \\ &\quad \times \beta(\mathbf{x}_k) \prod_{\substack{n'=1 \\ n' \neq n}}^{N_k^{(j)}} \alpha(\mathbf{y}_{k,n'}^{(j)})d\mathbf{C}_{\epsilon,k}^{(j)}d\mathbf{x}_k\end{aligned}\quad (7)$$

where  $\sum_{\mathbf{y}_k^{(j)} \setminus \mathbf{y}_{k,n}^{(j)}}$  denotes ‘‘marginalizing out’’ all elements of  $\mathbf{y}_k^{(j)}$  except for  $\mathbf{y}_{k,n}^{(j)}$ . Note that the messages in (5)-(7) all involve ‘‘marginalizing out’’  $\mathbf{y}_k^{(j)}$ , the dimension of which grows linearly with the number of PFs. The complexity of this operation scales exponentially with the number of PFs. We observe that, due to the functional form of  $f(\mathbf{z}_k^{(j)}|\mathbf{x}_k, \mathbf{y}_k^{(j)}, \mathbf{C}_{\epsilon,k}^{(j)})$ , these measurement update messages are a mixture of zero-mean complex Gaussian PDFs of  $\mathbf{z}_k^{(j)}$ . To avoid the high computational complexity, we approximate each of these messages by a single zero-mean complex Gaussian PDF of  $\mathbf{z}_k^{(j)}$  [12]. In particular, we calculated the following approximate messages:  $\tilde{\iota}(\mathbf{x}_k; \mathbf{z}_k^{(j)}) = \mathcal{CN}(\mathbf{z}_k^{(j)}; \mathbf{0}, \mathbf{C}_{\iota,k}^{(j)})$ ,  $\tilde{\nu}(\mathbf{C}_{\epsilon,k}^{(j)}; \mathbf{z}_k^{(j)}) =$

$\mathcal{CN}(\mathbf{z}_k^{(j)}; \mathbf{0}, \mathbf{C}_{\nu,k}^{(j)})$ , and  $\tilde{\kappa}(\mathbf{y}_{k,n}^{(j)}; \mathbf{z}_k^{(j)}) = \mathcal{CN}(\mathbf{z}_k^{(j)}; \mathbf{0}, \mathbf{C}_{\kappa,k,n}^{(j)})$ . The covariance matrices  $\mathbf{C}_{\iota,k}^{(j)}$ ,  $\mathbf{C}_{\nu,k}^{(j)}$ , and  $\mathbf{C}_{\kappa,k,n}^{(j)}$  are computed via moment matching, i.e., they are the covariance of the original BP messages in (5)-(7). The computational complexity of calculating these covariance matrices scales only linearly with the number PFs (see [12] for details).

### B. Belief Calculation, State Declaration and Estimation

With the BP messages computed as discussed in Sec. III-A, beliefs can be obtained as

$$\begin{aligned}\tilde{f}(\mathbf{x}_k) &\propto \beta(\mathbf{x}_k) \prod_{j=1}^J \tilde{\iota}(\mathbf{x}_k; \mathbf{z}_k^{(j)}) \\ \tilde{f}(\mathbf{y}_{k,n}^{(j)}) &\propto \alpha(\mathbf{y}_{k,n}^{(j)})\tilde{\kappa}(\mathbf{y}_{k,n}^{(j)}; \mathbf{z}_k^{(j)}) \\ \tilde{f}(\mathbf{C}_{\epsilon,k}^{(j)}) &\propto \xi(\mathbf{C}_{\epsilon,k}^{(j)})\tilde{\nu}(\mathbf{C}_{\epsilon,k}^{(j)}; \mathbf{z}_k^{(j)}).\end{aligned}\quad (8)$$

These beliefs are computed using particles by following the importance sampling principle, with  $\beta(\mathbf{x}_k)$ ,  $\alpha(\mathbf{y}_{k,n}^{(j)})$ , and  $\xi(\mathbf{C}_{\epsilon,k}^{(j)})$ , respectively, used as the proposal PDFs [23]. To determine the number of PFs at each time step, a PF is declared to exist if its existence probability  $\tilde{f}(r_{k,n}^{(j)} = 1)$ , which computed from  $\tilde{f}(\mathbf{y}_{k,n}^{(j)})$ , is larger than a threshold  $T_{\text{dec}}$ .

The agent and existing PF positions are finally estimated based on minimum mean square error (MMSE) estimation [24], i.e.,

$$\begin{aligned}\hat{\mathbf{p}}_k &= \int \mathbf{p}_k \tilde{f}(\mathbf{p}_k) d\mathbf{x}_k \\ \hat{\mathbf{p}}_{k,n}^{(j)} &= \int \mathbf{p}_{k,n}^{(j)} \tilde{f}(\mathbf{p}_{k,n}^{(j)} | r_{k,n}^{(j)} = 1) d\mathbf{p}_{k,n}^{(j)}\end{aligned}$$

where  $\tilde{f}(\mathbf{p}_k)$  and  $\tilde{f}(\mathbf{p}_{k,n}^{(j)} | r_{k,n}^{(j)} = 1)$  can be obtained by marginalizing from  $\tilde{f}(\mathbf{x}_k)$  and  $\tilde{f}(\mathbf{y}_{k,n}^{(j)})$ , respectively.

The number of PFs increases with time. To limit computational complexity, we prune PFs, i.e., remove them from the state space if their existence probability is smaller than  $T_{\text{pru}}$ .

## IV. SIMULATION RESULTS

We consider a 2-D indoor localization scenario with  $J = 2$  PAs. The floor plan, positions of PAs, and the agent’s trajectory with 679 time steps are depicted in Fig. 4. The number propagation paths and their corresponding VAs are computed based on ray tracing [25], [26]. At each time step, the radio signal received by each PA is generated following (2). Only propagation paths and corresponding VAs that reflect from a single surface are considered. We set  $M = 41$  and  $\Delta = 10$  MHz, which corresponds to 400 MHz signal bandwidth and a maximum range of 30m. In total, 100 simulations are performed. We assume that the measurement noise  $\epsilon_k^{(j)}$  is independent and identically distributed (i.i.d.) across  $m \in \{1, \dots, M\}$ , leading to  $\mathbf{C}_{\epsilon,k}^{(j)} = \sigma_{\epsilon,k}^{(j)2} \mathbf{I}_M$ . The state transition PDFs  $f(\mathbf{x}_k|\mathbf{x}_{k-1})$ ,  $f(\phi_{k,n}^{(j)}|\phi_{k,n-1}^{(j)})$ , and  $f(\sigma_{\epsilon,k}^{(j)2}|\sigma_{\epsilon,k-1}^{(j)2})$  follow a constant-velocity model  $\mathbf{x}_k = \mathbf{F}\mathbf{x}_{k-1} + \mathbf{W}\mathbf{q}_{\mathbf{x},k}$  [27,

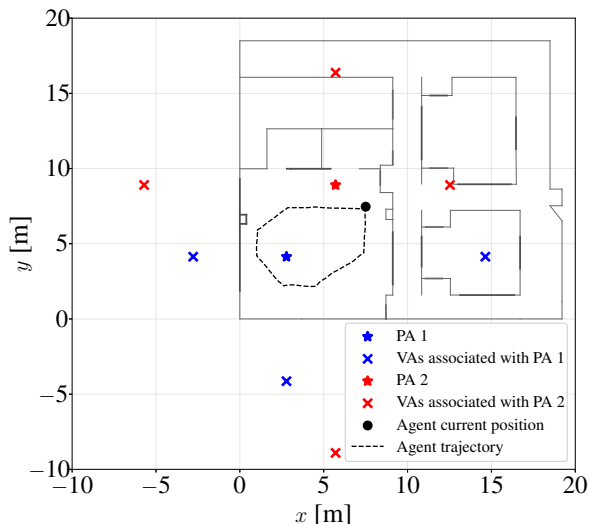


Fig. 4: Floor plan used for simulation. Agent and VAs positions for time step  $k = 1$  are shown.

Ch. 4], random walk model  $\phi_k^{(j)} = \phi_{k-1}^{(j)} + \mathbf{q}_{\phi,k}^{(j)}$ , and a Gamma distribution  $\mathcal{G}(\sigma_{\epsilon,k}^{(j)2}; \sigma_{\epsilon,k-1}^{(j)2}/c_\epsilon, c_\epsilon)$ , respectively. The covariance of  $\mathbf{q}_{\mathbf{x},k}$  and  $\mathbf{q}_{\phi,k}^{(j)}$  are set to  $\Sigma_{\mathbf{q},\mathbf{x}} = 10^{-4}\mathbf{I}_2$  and  $\Sigma_{\mathbf{q},\phi} = \text{diag}(10^{-8}, 10^{-8}, 10^{-4})$ , and we set  $c_\epsilon = 10$ . We set the declaration threshold to  $T_{\text{dec}} = 0.5$ , the pruning threshold to  $T_{\text{pru}} = 10^{-2}$ , the survival probability to  $p_s = 0.999$ , and the birth probability to  $p_{\text{B},n}^{(j)} = 10^{-4}$ .

We compare our proposed ‘‘Direct-SLAM’’ method with the state-of-the-art ‘‘BP-SLAM’’ method [1]. The reference method uses the MPC estimates from a snapshot-based parametric sparse Bayesian learning channel estimator [7]–[10] as measurements. The reference method uses the particle-based nonparametric BP method in [15], [16]. Fig. 5a shows the root mean square error (RMSE) of the agent position, and Fig. 5b shows their empirical cumulative distribution functions (CDFs). It can be seen that Direct-SLAM significantly outperforms BP-SLAM. The large RMSE of the agent position, e.g., around  $k \in [200, 400]$ , is related to a challenging geometry where multiple PFs have a similar propagation delay. As a result of this geometry, the channel estimator needed for BP-SLAM cannot accurately extract MPCs, i.e., due to finite resolution capabilities limited by signal bandwidth, fewer MPCs than actual signal components are extracted. The performance of the proposed Direct-SLAM method, which does not rely on a channel estimator, suffers less severely in this challenging geometry. Fig. 6 shows the generalized optimal sub-pattern assignment (GOSPA) error [28] of PFs with cutoff parameter  $c = 2$ , order  $p = 1$ , indicating that Direct-SLAM also achieves superior mapping accuracy compared to BP-SLAM.

## V. CONCLUSION

We propose a belief propagation (BP)-based method for multipath-based simultaneous localization and mapping (SLAM) that uses received radio signals as measurements. By avoiding the use of a channel estimator as a preprocess-

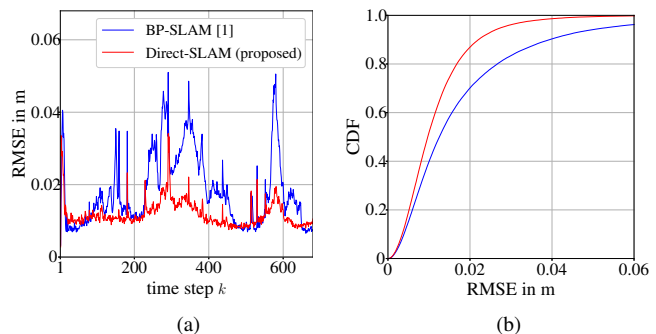


Fig. 5: (a) RMSE of the estimated agent position versus time step  $k$  over 100 simulation runs and (b) empirical CDFs of the RMSEs.

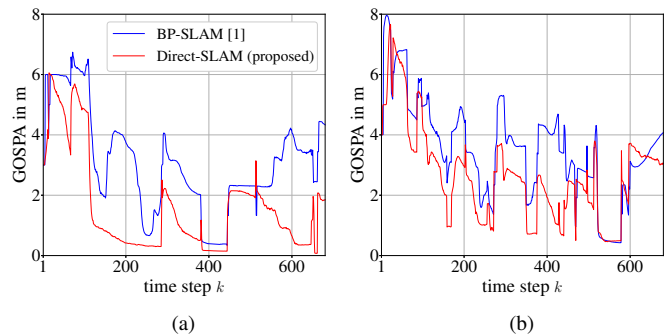


Fig. 6: GOSPA error of estimated PFs associated with (a) PA 1 and (b) PA 2 averaged over 100 simulation runs.

ing stage, the proposed approach can better exploit location information in received radio signals and thus succeed in geometrically challenging environments. For direct multipath-based SLAM, we introduced a new statistical model to describe the data-generating process of received radio signals, combining the Swerling 1 model for correlated measurements and a Bernoulli existence model. A factor graph is constructed based on the new statistical model. This factor graph provides the blueprint for developing an efficient BP method for direct multipath-based SLAM. For an accurate approximation, some of the BP messages are represented by random samples ‘‘particles’’ and others by a mean and covariance matrix obtained via moment matching. Performance evaluation is conducted based on synthetic data in a realistic scenario. It is demonstrated that the proposed method outperforms a state-of-the-art conventional method that relies on preprocessing of the received radio signal using a snapshot-based channel estimator. Future research avenues include BP-based processing that is neural enhanced [29] or has an embedded particle flow [30]–[33] as well as a representation of environmental features that enables data fusion [34].

## ACKNOWLEDGEMENT

The material presented in this work was supported by the Under Secretary of Defense for Research and Engineering under Air Force Contract No. FA8702-15-D-0001 and by Qualcomm Innovation Fellowship No. 492866.

## REFERENCES

- [1] E. Leitinger, F. Meyer, F. Hlawatsch, K. Witrisal, F. Tufvesson, and M. Z. Win, "A belief propagation algorithm for multipath-based SLAM," *IEEE Trans. Wireless Commun.*, vol. 18, Dec. 2019.
- [2] R. Mendrzik, F. Meyer, G. Bauch, and M. Z. Win, "Enabling situational awareness in 5G millimeter wave massive MIMO systems," *IEEE J. Sel. Topics Signal Process.*, vol. 13, pp. 1196–1211, Sept. 2019.
- [3] E. Leitinger, S. Grebien, and K. Witrisal, "Multipath-based SLAM exploiting AoA and amplitude information," in *Proc. IEEE ICC-19*, (Shanghai, China), May 2019.
- [4] F. Meyer and K. L. Gemba, "Probabilistic focalization for shallow water localization," *J. Acoust. Soc.*, vol. 150, no. 2, pp. 1057–1066, 2021.
- [5] C. Gentner, T. Jost, W. Wang, S. Zhang, A. Dammann, and U.-C. Fiebig, "Multipath assisted positioning with simultaneous localization and mapping," *IEEE Trans. Wireless Commun.*, vol. 15, pp. 6104–6117, June 2016.
- [6] S. Kadambi, A. Behboodi, J. B. Soriaga, M. Welling, R. Amiri, S. Yerramalli, and T. Yoo, "Neural RF SLAM for unsupervised positioning and mapping with channel state information," in *Proc. IEEE ICC-22*, pp. 3238–3244, Aug. 2022.
- [7] D. Shutin, W. Wang, and T. Jost, "Incremental sparse Bayesian learning for parameter estimation of superimposed signals," in *Proc. SampTA-13*, pp. 6–9, Sept. 2013.
- [8] P. Gerstoft, C. F. Mecklenbräuker, A. Xenaki, and S. Nannuru, "Multisnapshot sparse Bayesian learning for DOA," *IEEE Signal Process. Lett.*, vol. 23, pp. 1469–1473, Aug. 2016.
- [9] T. L. Hansen, B. H. Fleury, and B. D. Rao, "Superfast line spectral estimation," *IEEE Trans. Signal Process.*, vol. 66, pp. 2511–2526, Feb. 2018.
- [10] S. Grebien, E. Leitinger, K. Witrisal, and B. H. Fleury, "Super-resolution estimation of UWB channels including the diffuse component—An SBL-inspired approach," 2023, submitted.
- [11] A. Lepoutre, O. Rabaste, and F. Le Gland, "Multitarget likelihood computation for track-before-detect applications with amplitude fluctuations of type Swerling 0, 1, and 3," *IEEE Trans. Aerosp. Electron. Syst.*, vol. 52, pp. 1089–1107, June 2016.
- [12] M. Liang, T. Kropfreiter, and F. Meyer, "A BP method for track-before-detect," *IEEE Signal Process. Lett.*, vol. 30, pp. 1137–1141, 2023.
- [13] H.-A. Loeliger, "An introduction to factor graphs," *IEEE Signal Process. Mag.*, vol. 21, no. 1, pp. 28–41, 2004.
- [14] F. R. Kschischang, B. J. Frey, and H.-A. Loeliger, "Factor graphs and the sum-product algorithm," *IEEE Trans. Inf. Theory*, vol. 47, pp. 498–519, Feb. 2001.
- [15] F. Meyer, O. Hlinka, H. Wymeersch, E. Riegler, and F. Hlawatsch, "Distributed localization and tracking of mobile networks including noncooperative objects," *IEEE Trans. Signal Inf. Process. Netw.*, vol. 2, pp. 57–71, Mar. 2016.
- [16] F. Meyer, P. Braca, P. Willett, and F. Hlawatsch, "A scalable algorithm for tracking an unknown number of targets using multiple sensors," *IEEE Trans. Signal Process.*, vol. 65, pp. 3478–3493, July 2017.
- [17] F. Meyer, T. Kropfreiter, J. L. Williams, R. Lau, F. Hlawatsch, P. Braca, and M. Z. Win, "Message passing algorithms for scalable multitarget tracking," *Proc. IEEE*, vol. 106, pp. 221–259, Feb. 2018.
- [18] P. Meissner, *Multipath-Assisted Indoor Positioning*. PhD thesis, Graz University of Technology, 2014.
- [19] M. I. Skolnik, *Introduction to Radar Systems*. New York: McGraw-Hill, 3rd ed., 2002.
- [20] A. Richter, *Estimation of Radio Channel Parameters: Models and Algorithms*. PhD thesis, Ilmenau University of Technology, 2005.
- [21] J. Salmi, A. Richter, and V. Koivunen, "Detection and tracking of MIMO propagation path parameters using state-space approach," *IEEE Trans. Signal Process.*, vol. 57, pp. 1538–1550, Apr. 2009.
- [22] E. Leitinger, S. Grebien, B. H. Fleury, and K. Witrisal, "Detection and estimation of a spectral line in MIMO systems," in *Proc. Asilomar-20*, pp. 1090–1095, Oct. 2020.
- [23] M. S. Arulampalam, S. Maskell, N. Gordon, and T. Clapp, "A tutorial on particle filters for online nonlinear/non-Gaussian Bayesian tracking," *IEEE Trans. Signal Process.*, vol. 50, pp. 174–188, Feb. 2002.
- [24] S. M. Kay, *Fundamentals of Statistical Signal Processing: Estimation Theory*. Upper Saddle River, NJ: Prentice-Hall, 1993.
- [25] J. Borish, "Extension of the image model to arbitrary polyhedra," *J. Am. Statist. Assoc.*, vol. 75, pp. 1827–1836, Mar. 1984.
- [26] F. Antonio, "Iv.6 - faster line segment intersection," in *Graphics Gems III*, pp. 199–202, San Francisco: Morgan Kaufmann, 1992.
- [27] Y. Bar-Shalom, T. Kirubarajan, and X.-R. Li, *Estimation with Applications to Tracking and Navigation*. New York, NY: Wiley, 2002.
- [28] A. S. Rahmathullah, Á. F. García-Fernández, and L. Svensson, "Generalized optimal sub-pattern assignment metric," in *Proc. FUSION-17*, pp. 1–8, July 2017.
- [29] M. Liang and F. Meyer, "Neural enhanced belief propagation for multiobject tracking," *IEEE Trans. Signal Process.*, vol. 72, pp. 15–30, Sept. 2023.
- [30] L. Dai and F. Daum, "On the design of stochastic particle flow filters," *IEEE Trans. Aerosp. Electron. Syst.*, vol. 59, no. 3, pp. 2439–2450, 2023.
- [31] W. Zhang and F. Meyer, "Multisensor multiobject tracking with high-dimensional object states," 2023, submitted.
- [32] J. Jang, F. Meyer, E. R. Snyder, S. M. Wiggins, S. Baumann-Pickering, and J. A. Hildebrand, "Bayesian detection and tracking of odontocetes in 3-D from their echolocation clicks," *J. Acoust. Soc.*, vol. 153, no. 5, pp. 2690–2705, 2023.
- [33] L. Wielandner, E. Leitinger, F. Meyer, and K. Witrisal, "Message passing-based 9-D cooperative localization and navigation with embedded particle flow," *IEEE Trans. Signal Inf. Process. Netw.*, vol. 9, pp. 95–109, Jan. 2023.
- [34] E. Leitinger, A. Venus, B. Teague, and F. Meyer, "Data fusion for multipath-based SLAM: Combining information from multiple propagation paths," *IEEE Trans. Signal Process.*, vol. 71, pp. 4011–4028, 2023.